Performance Study of the CMS Ecal Electronics using electrons from 15 GeV to 250 GeV

S. Argirò[a] for the CMS ECAL group

[a] University of Torino and INFN, Italy

stefano.argiro@to.infn.it

Abstract

The experimental conditions and physics goals of LHC experiments set challenging specifications for detectors and their readout electronics. The CMS Electromagnetic Calorimeter (Ecal) is an example of a complex system in which every component needs to be understood in detail in order to ensure the quality of the physics results. In 2006, 9 ECAL supermodules were exposed to an electron test beam in the energy range from 15 GeV and 250 GeV. Many aspects of the calorimeter response have been studied in detail. We will describe the results of these studies, with emphasis on the contribution of the electronics to linearity, resolution and noise of the system.

I. Introduction

In 2006, 8 of the 36 supermodules of the CMS Electromagnetic Calorimeter (ECAL) barrel were exposed to the Cern H4 electron beam with energy ranging from 15 to 250 GeV. The supermodules were in their final configuration. The primary goal of the test beam campaign was to provide an accurate relative calibration of the ECAL channels, but it was also an opportunity to carry several performance studies, some of which concerned in particular the readout electronics.
One additional ECAL barrel supermodule was exposed to the H2 beam, where it was irradiated with pions and electrons of energies between 1 and 10 GeV, while all the supermodules accumulated significant cosmic muon data using a third test setup. Among the studies that were performed at the H4 test facility, we will mention shower containment, position resolution, and the ones that we will report about, i.e. response linearity, energy resolution and noise.

II. Description of the ECAL

The CMS ECAL [3] is built of a barrel and two endcaps. The barrel comprises 61200 $PbWO_4$ (lead tungstate) crystals arranged in a quasi-projective geometry, and use avalanche photodiodes (APD) as the photosensitive device. The material was chosen for its fast scintillation time, high radiation tolerance, and short radiation length, while the photodetector was chosen for its ability to operate in a magnetic field (the ECAL is placed inside the CMS solenoid). The endcap is made of four "dees", each comprising 7324 crystals equipped with vacuum photo-triodes (VPT), chosen for the superior radiation hardness required in the forward region.

A. Design performance

The ECAL was built to give the experimenters the potential for the discovery of a narrow Higgs resonance, keeping in mind the fact that a light Higgs would have a very narrow decay width to 2 photons. Therefore an excellent energy resolution is required. The design energy resolution was parametrized in the form

$$\frac{\sigma}{E} = \frac{2.7\%}{\sqrt{E}} + 0.5\% + \frac{150MeV}{E}$$

where the values of the parameters are the ones of the reference design for low luminosity. The first term is connected to photostatistics and shower containment, the second to calibration and non-uniformity, while the third one carries the contribution of the noise of the electronics.

B. Readout electronics

From the point of view of the electronics, the building block of the calorimeter is the so called "trigger tower", made of a matrix of 5×5 crystals. Each row of five is connected to a very front end card (VFE) that provides signal shaping, amplification and digitization, while five VFE cards are connected to a front end (FE) card that performs trigger primitive generation and readout. The FE card is the last of the on-detector components, data being sent off-detector via Gigabit optical links.

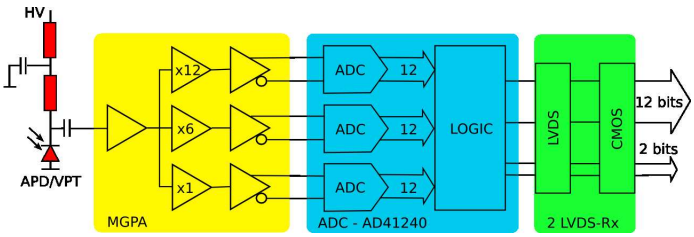

Figure 1: Schematics of the Very Front End card

The channel schematic implemented on the VFE card is depicted in figure 1. Details of the production and testing of these boards are presented in this conference by Jan Blaha [4]. The signal from the APD or the VFE is processed by a preamplifier with a shaping time of 40 ns. Then the signal is amplified with three different gains, nominally 12,6 and 1. The above stages are implemented on a custom ASIC called Multi Gain Pre Amplifier (MGPA), while on a separate chip they are sampled at 40 Mhz by three 12 bit ADCs. Logic circuits select the highest non-saturated sample in each time slice, but once the signal

causes the switch to lower gain, the gain itself is not set back to the previous value for 5 samples, even if it returned to the higher gain range. The total dynamic range achieved is 15 bit.

C. VFE specifications and bench tests

Table 1 reports the design parameters of the MGPA chip. The result of bench tests were reported in previous works [1]. The non-linearity measurement is reported in figure 2 and is within specifications. The noise on the bench was found to be around 8000e, or 1.28fC, also within specifications.

Fullscale signal	60 pC
noise ENC	10k e (1.6 fC)
output signals	1.8V
pulse shaping	40 ns
nonlinearity	< 0.1 % fullscale

Table 1: Design performances of the MGPA chip

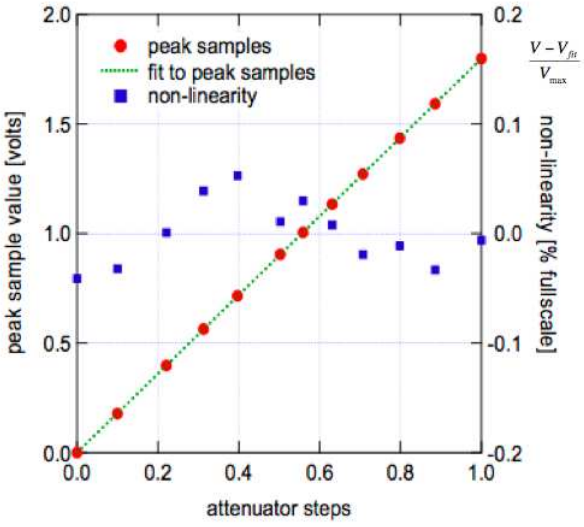

Figure 2: VFE linearity measured on the bench

III. Data Analysis

In this section we will review the methods used to analyze the data coming from the H4 test beam campaign.

A. Setup of the Test Beam

The supermodule under study was placed on a turntable that allowed the beam to be centered on a particular crystal. Along the H4 beamline several scintillators were installed to provide the trigger and measure electron rates. Additionally, four planes of scintillating fibers could measure the beam position with a resolution of about 150 μm. The run period lasted about 70 days, with more than 2 $\times 10^9$ triggers recorded.

B. Signal Reconstruction

Given the digitized signal coming from the crystals, a digital filtering technique is applied to reconstruct the amplitude A and the peaking time T_{max} (figure 3). The amplitude, for example is estimated using the formula

$$A = \sum_{i=1}^{N} w_i S_i$$

where S_i is the i^{th} sample and w_i is a weight derived from the knowledge of the pulse shape (see [2] for details). At LHC, the phase between the clock and the ECAL signal will be constant, since the experiment clock will be synchronized with bunch crossing. This was not the case during the test beam were, for example, the peak of the signal from the calorimeter could fall at any position between two clock ticks. For this reason, a single set of weights is not sufficient. We therefore divided each interval between clock ticks in 25 bins of 1ns each and derived 25 different sets of weights. The information about which set was to be used (the phase between clock and trigger) came from a TDC connected to one of our trigger scintillators.
For each signal completely in gain 12, we used eight samples, three on the pedestal and 5 on the signal. This method was found to give the best signal to noise ratio and there is no need to measure pedestals separately. For signals in gain 6, four samples on the signal were used, while for pedestal estimation one has to rely on pedestal runs, since, because of the gain switch, there is no information about the pedestal in this range in the samples.

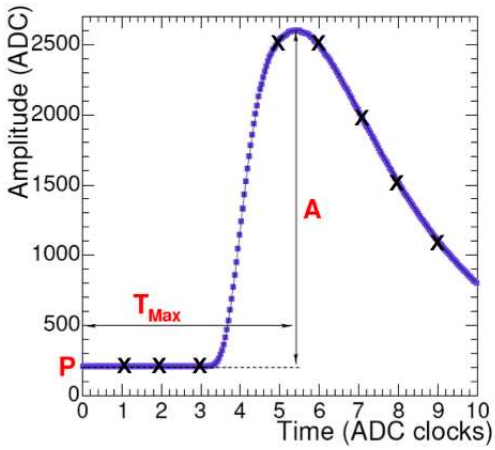

Figure 3: Example of a digitized pulse

C. Noise measurement

We measured the noise using pedestal runs, by calculating the RMS of the bare samples. We report the results in each gain for two supermodules in figure 4. Noise is very uniform across channels and the two supermodules behave very similarly.

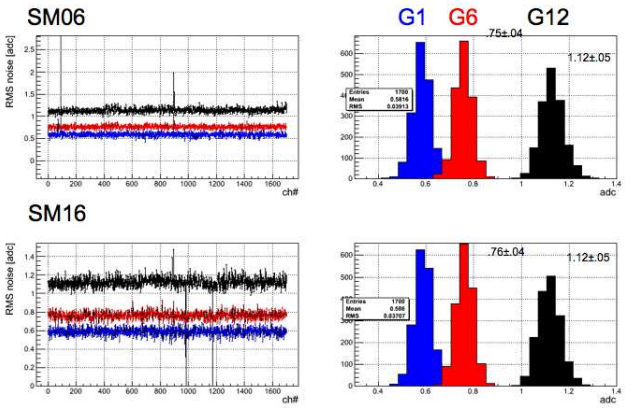

Figure 4: Left: RMS noise for each channel of two supermodules. From top to bottom the three curves refer to gain 12, 6, 1. Right: histogram of the RMS noise. From left to right, the three distributions represent gain 1, 6 and 12

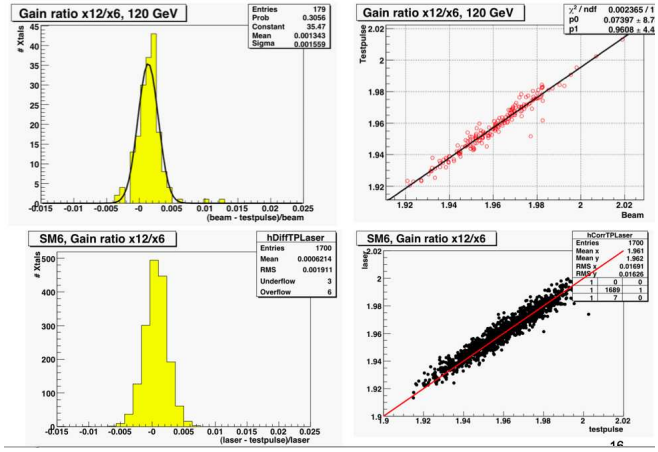

Figure 5: Difference and correlation between different methods of evaluating gain ratios. Top: difference between beam and testpulse. Bottom: Difference between laser and testpulse

We also measured the noise of the sums of 3×3 and 5×5 crystal matrices, as cluster reconstruction involves considering several crystals at once. The results are reported in table 2. It can be noted that there is no correlated noise across signals (the noise of the matrices is roughly equal to the sum of the noise in each crystal) and that the two supermodules are very similar.

	Noise SM16 [GeV]	Noise SM6 GeV
G12 1x1	36.5	36.5
G6 1x1	28.2	28.5
G12 3x3	107.5	104.9
G6 3x3	72.9	71.7
G12 5x5	179.9	174.0
G6 5x5	121.7	119.5

Table 2: The Energy Noise Equivalent in the sum of 1,9,25 crystals

D. Determination of gain ratios

We have already seen that each MGPA channel amplifies the signal with three different gains, to cover a dynamic range of 15 bit with a 12 bit ADC. It is therefore important to measure the ratios between these gains accurately, while the absolute measurement is given by the absolute energy scale of the calorimter, and will be determined using physics events such as electrons coming from Z or W decay.
Gain ratios for each MGPA channel can be determined in several ways. First, they can be measured using the internal charge injection system. A test charge is injected and measured in two of the three gains to measure their ratios. A second method consists in firing a laser pulse with the laser monitoring system. The last method makes use of electrons of a given energy, for example 120 GeV. Two consecutive runs are taken at two different gain settings, therefore allowing their ratio to be measured. These methods have been shown to give comparable and well correlated results. The difference in the gain ratio sets is at the per-mil level. These differences are shown in figure 5

E. Energy resolution and response linearity

A common analysis procedure is used to measure the linearity of the calorimeter response and the energy resolution. First the crystal with the highest energy deposit is selected for each event. Then the *maximum containment point* is estimated. This is point on the face of the crystal that corresponds to the highest fraction of the shower being contained in that crystal. Only electrons that fall within an area of $4mm^2$ around the maximum containment point are selected, to avoid effects due to shower containment. For each beam energy, the energy (in the 5×5 matrix) spectrum of these electrons is fit with a function which is the sum of a gaussian and an exponential to take into account the low energy tail. The graph of beam energy versus reconstructed energy is then fit with a linear function, and deviations from the fit are used to produce the plot of figure 6. The maximum deviation from linearity is of the order of 0.25%.

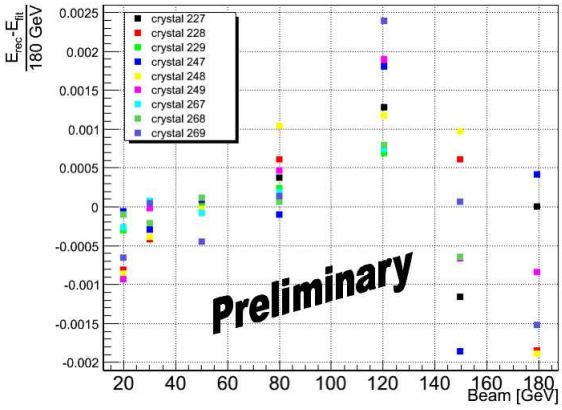

Figure 6: Differential non-linearity of supermodule 16. The maximum deviation from linearity does not exceed 0.25%

In a similar manner, for each energy point the width σ of the reconstructed energy distribution is used to plot the energy

resolution $\frac{\sigma}{E}$, as in figure 7.

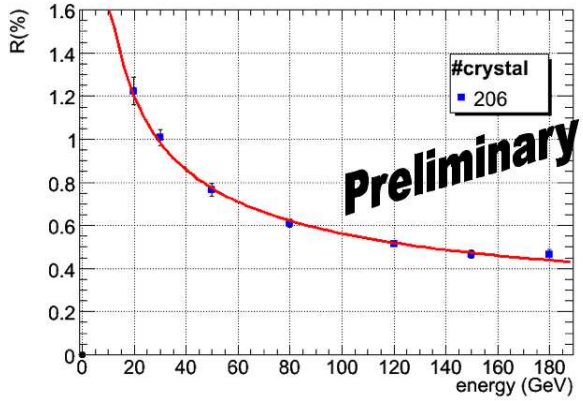

Figure 7: Energy resolution of crystal 206 in supermodule 16

Figure 8 reports again the plot of energy resolution versus energy, but with many channels on the same graph to show the low dispersion of the resolution curve. The stability of the results when changing cuts or fit function has been studied and proven to be very good.

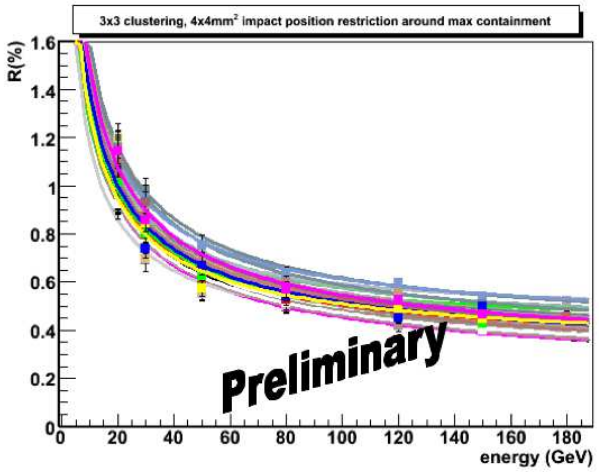

Figure 8: Energy resolution of several crystals in supermodule 16

The graph of $\left(\frac{\sigma}{E}\right)^2 - \left(\frac{N}{E}\right)^2$ versus $\frac{1}{E}$, where N is the noise parameter measured independently, is fit with a linear function to extract the statistical and constant term of the resolution function A..

A global fit to several channels gives a stochastic term of 3.50 ± 0.8 and 0.33 ± 0.01.

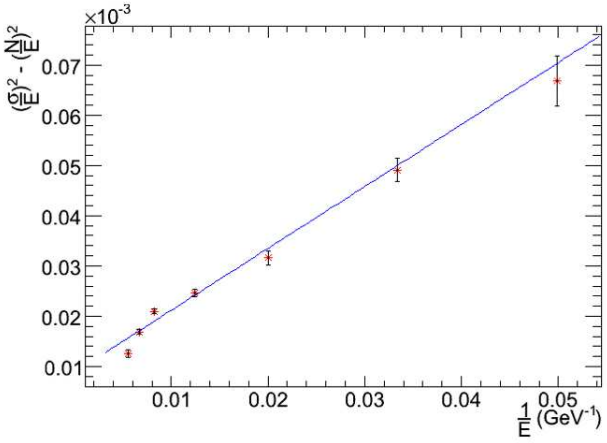

Figure 9: Plot used to extract the energy resolution parameters

IV. Conclusions

The CMS Ecal barrel has been extensively studied in different testbeam campaigns. Performances fulfil design specifications. In particulart he noise is around 110 MeV in the 3×3 matrix and 170 MeV in the 5×5 matrix, and is very uniform within and across supermodules.

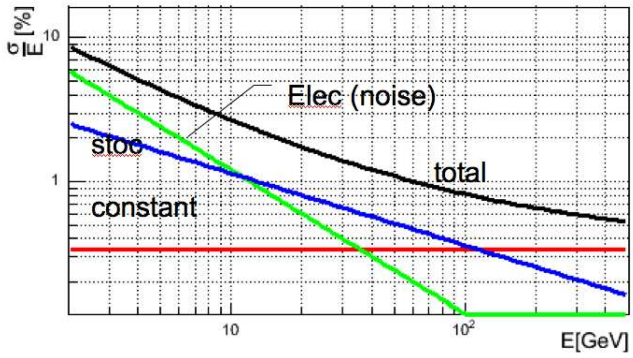

Figure 10: Contribution of stochastic, constant and noise term to the energy resolution. The resolution is parametrized as in A., but the values of the parameters are the ones measured at the test beam

The electronics behaved as expected. In particular, the contribution of the electronics noise to energy resolution becomes negligible after 10 GeV, as illustrated in figure 10, where the contribution of the various terms to energy resolution is shown. The parameters used for this plot are the ones measured with the test beam.

REFERENCES

[1] Raymond, M. et al., "The MGPA electromagnetic calorimeter readout chip for CMS", IEEE Trans. Nucl. Sci. 52 2005,756-763

[2] Bruneliere, R. and Zabi, A., " Reconstruction of the signal amplitude of the CMS electromagnetic calorimeter", CERN-CMS-NOTE-2006-037, Feb 2006.

[3] CMS collaboration, "CMS ECAL Technical Design Report", CERN/LHCC 97-33, 15 December 1997

[4] Blaha, J., "Calibration and performance tests of the Very-Front-End electronics for the CMS electromagnetic calorimeter", this conference